Pulsating Laminar Flow Measurements with a Directionally Sensitive Laser Velocimeter

EARLY B. DENISON, WARREN H. STEVENSON, and ROBERT W. FOX

School of Mechanical Engineering
Purdue University, Lafayette, Indiana 47906

SCOPE

The laser Doppler velocimeter provides a method for measuring local velocities in a gas or liquid without the insertion of a disturbance-producing probe into the flow field. Probes are particularly disadvantageous in unsteady flows, which occur frequently in engineering problems requiring detailed velocity measurements.

The present investigation was undertaken with two primary objectives in mind: to explore the capabilities and limitations of a laser velocimeter for time-dependent measurements and to make detailed velocity measurements in a well-defined unsteady flow. Specifically, the laminar pulsatile flow of an incompressible Newtonian fluid in a rigid circular tube was investigated with a directionally sensitive laser velocimeter which was capable of measuring local velocities at points across the tube (radially) and along the tube axis. Measurements are reported for $N_{Re} \approx 1000$, $4 \leq \beta \leq 6$, $\overline{Q} \approx 0.16$, and $0.025 \leq z^* \leq 0.35$. N_{Re} the Reynolds number based on the mean flow rate, β is the frequency-viscosity parameter (a pseudo Reynolds number), $\overline{Q}$ is the ratio of the maximum unsteady flow rate to the mean flow rate, and z^* is the dimensionless distance from the tube entrance.

Almost all previously reported measurements with laser velocimeters have been limited to steady laminar flows or to simple turbulence intensity determination. Velocity measurements in pulsatile laminar flows have been made by a number of investigators, but to date all of the data have been obtained by instruments requiring the presence of a probe in the flow field. These pulsatile flow results have often differed from the analytical predictions of Uchida (*20*) for the fully developed region and Atabek and Chang (*3*) for the developing flow region.

SUMMARY

Although the experience gained in this study is restricted to one specific laser velocimeter system, it provides a good basis for an understanding of the technique and for determining its suitability for use in various situations. The unit naturally has certain limitations (velocity range, spatial resolution, etc.), but many of them may be removed by relatively simple modifications. Effective beam diameter at the scattering volume (which is related to the volume over which the fluid velocity is being measured) was shown to be about six times the calculated diffraction limited spot size. This enlargement was due primarily to aberrations introduced by the test section and its surrounding box. The frequency response characteristics of the system were not determined, but they were definitely impaired by the signal broadening encountered owing to the limited spatial resolution. Considerable improvement in system performance could be obtained by improving the optical design of the instrument. A study of this problem is currently under way.

In spite of the problems posed by optical effects in the test section, very accurate data were obtained for $|\overline{R}|$, the dimensionless tube radius, less than 0.6 under all flow conditions. The fully developed data agree with Uchida's solution well within the predicted uncertainty for $|\overline{R}| < 0.6$. [The center line uncertainty is 2.6% of the mean velocity (*13*).] The developing flow solution of Atabek and Chang slightly underpredicted the entrance length for the range of parameters under consideration. Because no loss of accuracy would be expected in the developing flow region, this small deviation from the solution is believed to be a real effect. To determine exactly why the Atabek and Chang analysis shows this deviation will require a detailed comparison between its predictions and those of other techniques.

PULSATILE FLOW IN A RIGID TUBE

A pulsatile flow consists of a mean flow with a superposed oscillatory component. This type of flow occurs in hydraulic lines and control systems, the circulation of the blood, intake and exhaust passages of internal combustion engines, and liquid propellant rocket engines. Much of the work done with pulsatile flow has been due to investigators interested in physiological considerations.

Uchida (*20*) analyzed the fully developed pulsatile flow of an incompressible Newtonian fluid in a circular tube. He presented an exact solution which allows computation of the velocity field from measurements of the pressure field. Atabek and Chang (*3*) analyzed pulsatile flow in the entrance region of a tube by making a number of simplifying approximations in the Navier-Stokes equations. Their solution, as used in the present investigation, requires a knowledge of the pressure gradient (to compute the fully developed solution) and the instantaneous flow rate (to compute the perturbation from the fully developed solution). Results of these analyses show that the unsteady

Correspondence concerning this article should be addressed to Dr. E. B. Denison, Shell Development Co., P.O. Box 481, Houston, Texas 77001.

(oscillatory) portion of a pulsatile flow velocity profile displays some very interesting behavior. The profile shape is characterized by the frequency-viscosity parameter, $\beta = R[\omega/\nu]^{1/2}$. Flows dominated by viscous effects are characterized by low values of β; inertially dominated flows (slug flows) are characterized by high values of β.

Previous pulsatile flow measurements have been made by hot-film anemometers (*4, 15*), pitot-static probes (*6*), and the hydrogen bubble technique (*12*). Various degrees of agreement with the theoretical solutions for both developing and fully developed flow have been shown. One objective of the present study was to verify or disprove the accuracy of the solutions.

LASER VELOCIMETER DESIGN CONSIDERATIONS

Yeh and Cummins (*21*) first demonstrated the use of the laser Doppler velocimeter in 1964 by investigating steady laminar flow in a pipe. Since that time many investigators have used the device for steady laminar flow measurements (*1, 5, 16,* and *18*) and a number have analyzed the performance of the instrument from a theoretical standpoint (*7, 11,* and *19*). Simple measurements (*17*) in a turbulent flow have been made and oscillatory flow measurements (*14*) have also been reported.

The operating principles of laser velocimeters have been thoroughly explained in the references mentioned. If one wishes to apply these general principles to a particular flow measurement problem, careful analysis of such factors as physical constraints, accuracy requirements, and optical properties of the flow must be made. Each flow situation will probably warrant individual consideration before an acceptable optical system can be designed. Of prime importance is the ease with which access can be obtained to the flow. Normally, the beams are focused to a location in the flow field so that localized velocity measurements may be made. The beam or beams must reach the point of interest with minimum distortion in order that the scattering volume be relatively small.

EXPERIMENTAL APPARATUS:

Optics

The basic optical configuration used in the present work is credited to Goldstein and Kreid (*18*) and has been modified slightly for directionally sensitive measurements (*14*). The system is shown in Figure 1. The angle between the two beams was chosen after considering three factors. First, the scattered beam intensity is dependent on this angle; it decreases rapidly as the angle increases for the particle size and radiation wavelength used in this investigation (*8*). Second, the spatial resolution of the instrument is degraded as the intersecting volume of the beams (scattering volume) is increased. This takes place as θ_f decreases ($\theta_f = \theta$ for this investigation, see Figure 2). Finally, the range of Doppler frequency shifts produced by the device for a given velocity range is dependent on the angle θ_f.

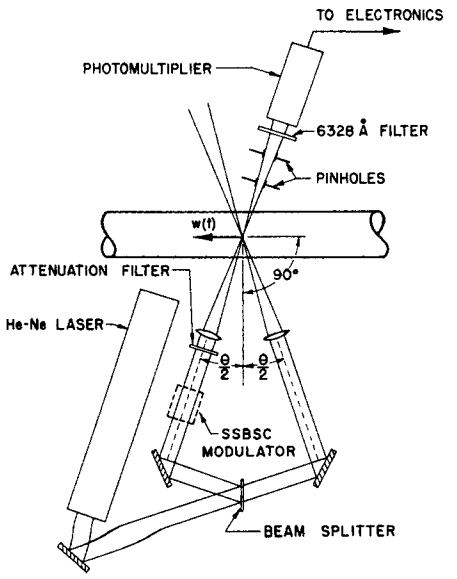

Fig. 1. Modified Goldstein-Kreid optical system.

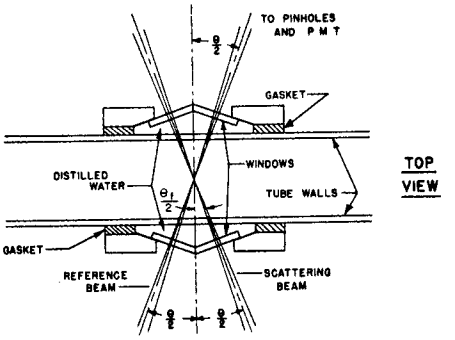

Fig. 2. Compensator box.

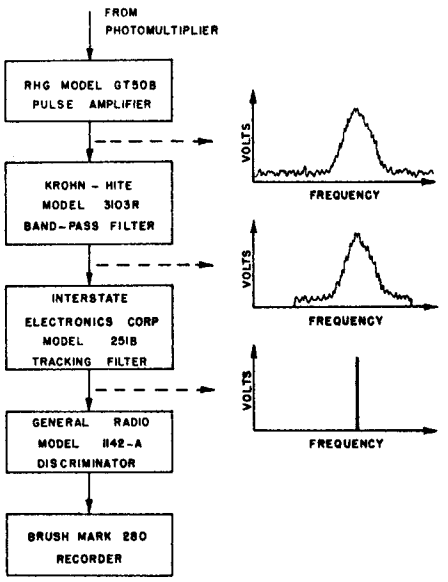

Fig. 3. Signal processing electronics.

Because the flow to be investigated was confined by curved walls and the fluid's refractive index was different from that of air, the light beams suffered aberrations before their intersection. The scattering volume was therefore enlarged. An elaborate optical design was not undertaken for the present investigation; however, a small compensator box was constructed and placed around the test section. The box had windows on both sides made from microscope slides and was filled with distilled water in an attempt to keep the refractive index nearly constant for the beams traversing the box and test section and to eliminate large refractions ($\theta = \theta_f$). This is shown in Figure 2. The glass tubing comprising the test section was not ground and polished on the outside diameter, and so slight irregularities in the surface existed. The compensator box minimized the effects of the irregularities and also the effects of beam misalignment with the curved tube wall. The optical path length in glass and water was increased by the addition of the box, however, so that the elimination of the large refraction angles was partially offset by the increased path length. Measurements showed that the scattering volume size was not significantly altered by the addition of the com-

pensator box, but the beam intensities exhibited much smaller fluctuations as the tube was traversed.

Ideally, the signal from a Doppler device is at a single frequency related to the velocity in the test section by

$$w = \frac{\Delta f_d \lambda_o}{2n \sin(\theta_f/2)} \tag{1}$$

However, in practice the signal is broadened by a number of effects. As the scattering volume is finite in size, velocity variations may exist in the volume and a signal consisting of a broadened spectrum centered at the frequency representing the mean velocity will result. If the radial velocity gradient is not near-constant across the scattering volume, the spectrum will be skewed (unsymmetrical). Also, θ_f is not actually a constant across the incident and scattered beams, for they have finite convergence and divergence angles, respectively. This angle variation yields another broadening effect. Additional broadening occurs due to the fact that the particles remain in the scattering volume for only a short period of time; their scattering signal is transmitted only briefly and a resultant "pulse modulation" occurs (*11*). These broadening effects must be taken into account in the data analysis.

As the effective scattering volume has such an important effect upon system performance, lenses with various focal lengths were tried in an attempt to minimize the scattering volume and the resulting output spectrum width. 193 mm. focal length lenses were finally employed as no apparent reduction in signal bandwidth was found at shorter focal lengths.

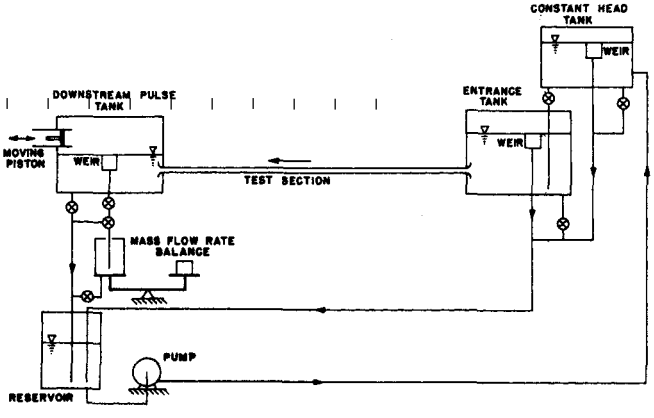

Fig. 4. Flow system.

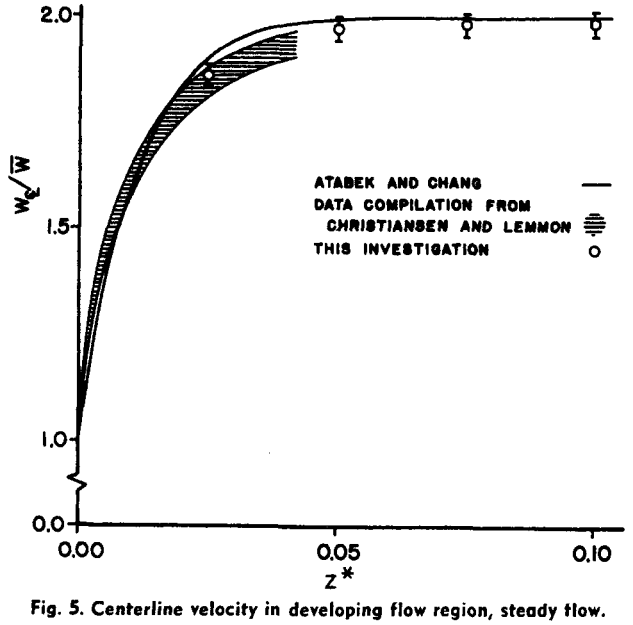

Fig. 5. Centerline velocity in developing flow region, steady flow.

With these lenses the effective beam diameter at $\overline{R} = 0.5$ was inferred from the measured spectrum width and the known velocity distribution for a fully developed steady laminar flow (*13*). It was shown that spectrum widening due to the velocity gradient dominated over the other widening effects. This effective beam diameter was measured to be about 540 μ compared to a calculated diffraction limited spot size of 90 μ at the same f/number. Data indicated that there was negligible change in the scattering volume size as the tube was radially traversed.

Electronics

In principle the signal processing should be simple, but in practice it turns out to be rather complex. If the photomultiplier (PMT) yields a beat frequency output that is linearly proportional to the velocity in the test section, then a frequency to voltage converter (discriminator) should complete the processing. A fundamental complication arises from the fact that photomultipliers are inherently noisy devices. Their output contains "white" noise which is difficult to eliminate, because one cannot operate in some different frequency range in an attempt to avoid it. Also, the desired beat signal itself is not a single frequency but has a characteristic frequency spectrum owing to the broadening effects mentioned. If the velocity is a function of time as in the present study, then the frequency spectrum is also time-dependent. Thus, a tunable band-pass filter cannot be used to reduce the noise for the case of an unsteady flow.

To overcome these problems, the electronics system shown in Figure 3 was used in the present investigation. The key item is the tracking filter. This filter is characterized by a loop bandwidth that is analogous to the bandwidth of a band-pass filter and it attempts to maximize the power within this band. The variable loop bandwidth was normally set at about 3 to 4% of the mean frequency shift for center-line measurements. This bandwidth was increased for measurements near the tube wall. The filter handled clean signals quite well, but as the spectrum broadened, owing to steep velocity gradients in the proximity of the tube walls, it became difficult for the device to locate the center frequency. In the present study the operation was satisfactory for $|\overline{R}| < 0.6$ under all flow conditions.

Flow System

The unsteady flow was produced by imposing a cyclic axial pressure gradient on the test section. A schematic of the complete flow system is shown in Figure 4. Liquid flowed from the constant level entrance tank through the test section and into the constant level downstream tank. The air above the working fluid in the downstream tank was periodically compressed and decompressed by means of a moving piston. This produced a varying pressure gradient in the test section and thus an unsteady flow. The piston was driven by a Scotch yoke powered by a Gerbing SCR Motor through Browning Gear Belts and Gears. Crankshaft speed was continuously monitored via a gear wheel-magnetic pickup-counter arrangement. The mass flow rate was monitored by a balance and electric timer combination.

The 30-ft.-long test section was made from accurately joined lengths of 0.750-in.-I.D. Pyrex Precision Bore glass tubing. It was aligned with a cathetometer and a target which could be moved from end to end inside the test section. No point along the entire length had its center more than 0.050 in. from the true center line. The entrance to the test section was an ASME Low β Series Long Nozzle (*2*).

Working fluid viscosity was varied in order to produce the desired flow parameters, β and N_{Re}. This was accomplished by mixing Pluracol V-10* and distilled water in a ratio of approximately 7.2:92.8 by weight. V-10 is an extremely viscous, high molecular weight, liquid polyoxyalkylene. The mixture had a kinematic viscosity near 6.6×10^{-5} sq.ft./sec. Tests run with a Fann VG Model 35 Rotational Viscometer indicated

* Manufactured by Wyandotte Chemical Corp., Wyandotte, Mich.

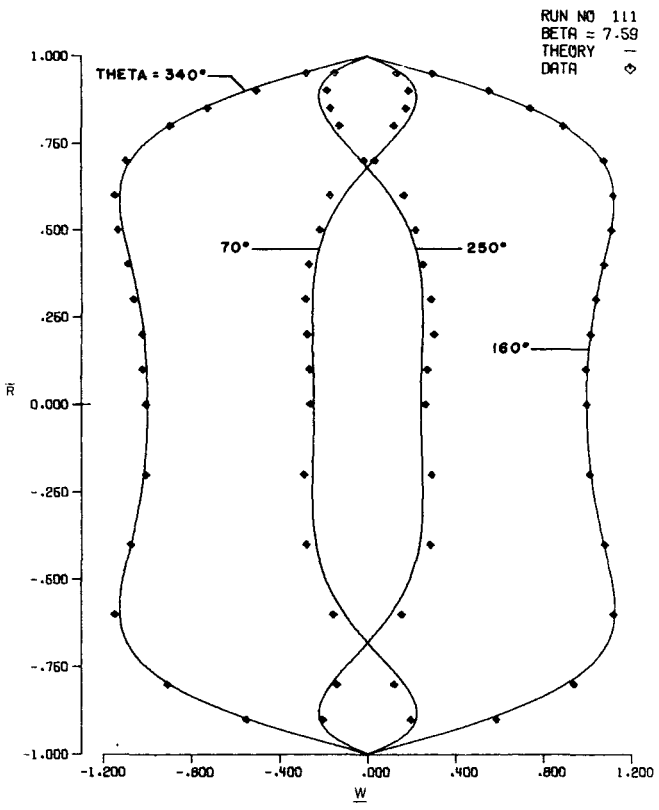

Fig. 6. Typical fully developed velocity profiles, oscillatory flow.

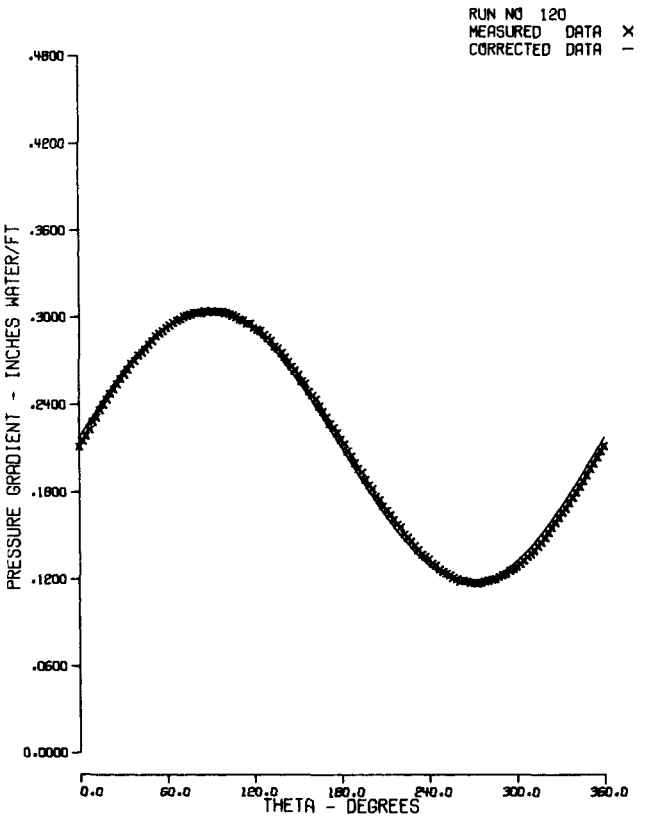

Fig. 7. Typical axial pressure gradient, pulsatile flow.

Newtonian behavior for shear rates to 1000 sec.$^{-1}$ (limit of the Model 35). The maximum shear rates encountered in the fully developed region of the flow were no more than 150 sec.$^{-1}$. Accurate viscosity measurements were obtained before each run with a Cannon-Fenske #150 Calibrated Routine Viscometer (capillary tube type) stabilized by a constant temperature circulator.

The scattering centers were 0.5-μ-diam. polystyrene latex* particles (specific gravity = 1.05), which can be shown to follow the flow with a high degree of accuracy (*13*). They were mixed with the working fluid in a ratio of from 1/50,000 to 1/30,000 by weight.

Computation of the fully developed velocity field requires a knowledge of either the instantaneous flow rate or the instantaneous axial pressure gradient. The axial pressure gradient was measured with a differential pressure transducer connected between static taps approximately 39 in. apart. Careful static and dynamic calibrations were performed on the transducer system before each data run.

DEVELOPING STEADY FLOW MEASUREMENTS

Steady flow measurements were made at four locations along the entrance region of the pipe. Velocity profiles were taken in order that the tube center line could be located by symmetry. These steady flow measurements were compared with the prediction of Atabek and Chang (*3*) as well as with data from other investigations.

Christiansen and Lemmon (*9*) have presented a theoretical solution for developing steady flow as well as a compilation of data from other investigations (both experimental and theoretical). Figure 5 shows a band inside of which the major portion of the data from Christiansen and Lemmon's compilation fall. The prediction of Atabek and Chang as well as the results of this investigation also are shown. The experimental uncertainty is shown for the data from this investigation (*13*). The solution of Atabek and Chang apparently predicts a premature development.

It should be pointed out that most flow systems do not produce a uniform velocity profile at the test section entrance. Theoretical solutions normally assume that the entrance profile is uniform across the pipe mouth. In order to make a valid comparison with existing data, a profile was measured at $z^* = 0.0056$ (physical constraints did not allow measurement at $z = 0$). Using the ratio of the measured center-line velocity to the measured mean velocity, along with the data compiled by Christiansen and Lemmon, it was shown that the fictitious entrance point corresponding to a uniform velocity profile should lie approximately 1.1 diameters outside the physical entrance (the throat of the entrance nozzle). For $N_{Re} \approx 1000$ and $z \geq 50\ R$, this creates a negligible change in z^*.

PULSATILE FLOW MEASUREMENTS

Pulsatile flow data were taken in both the fully developed and developing flow regions of the test section. $N_{Re} \approx 1000$, $\overline{Q} \approx 0.16$, $\beta \approx 4$, 5, 6, and $0.025 < z^* < 0.35$ is the range of parameters considered. The instantaneous pressure gradient was measured, digitized, Fourier analyzed, and corrected for the phase lag and amplitude distortion of the transducer system. These pressure measurements were made in the fully developed region for all data runs. The instantaneous flow rate was inferred from the pressure measurements using the compilation of Combs and Gilbrech (*10*). The viscosity, density, and frequency of pulsation were also measured. For each run velocity traces were taken at a dozen or more radial locations and digitized (36 points per cycle).

Four times during the cycle of pulsation, profiles were constructed from the measured data. One of the profiles

* Manufactured by Dow Chemical Co., Midland, Mich.

occurs near the time of maximum flow rate, one is near the minimum, while the remaining two are very near the mean or average flow rate. Combs and Gilbrech (*10*) have predicted the time (with respect to the pressure gradient) of maximum flow rate as a function of β. These times could not be exactly duplicated due to the finite sampling interval of the data, but they are very close. The theoretical solution was computed at the precise time at which the data was sampled.

Figure 6 shows a typical set of normalized velocity pro-

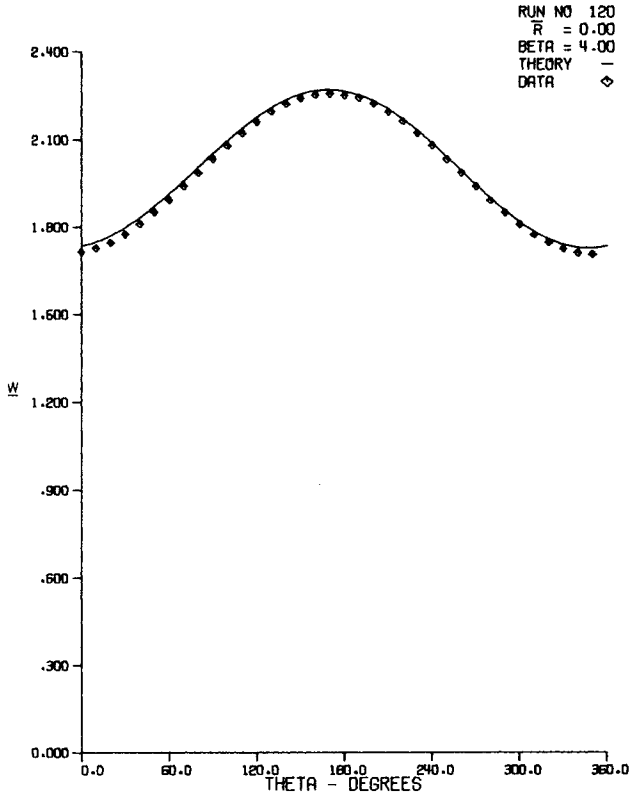

Fig. 8. Typical centerline velocity trace, fully developed pulsatile flow.

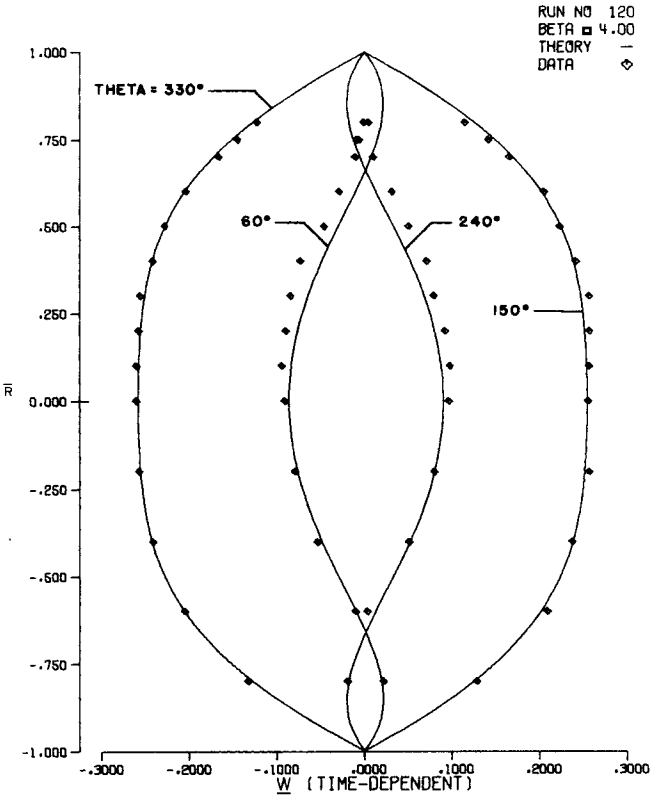

Fig. 10. Typical fully developed velocity profiles, unsteady component only, pulsatile flow.

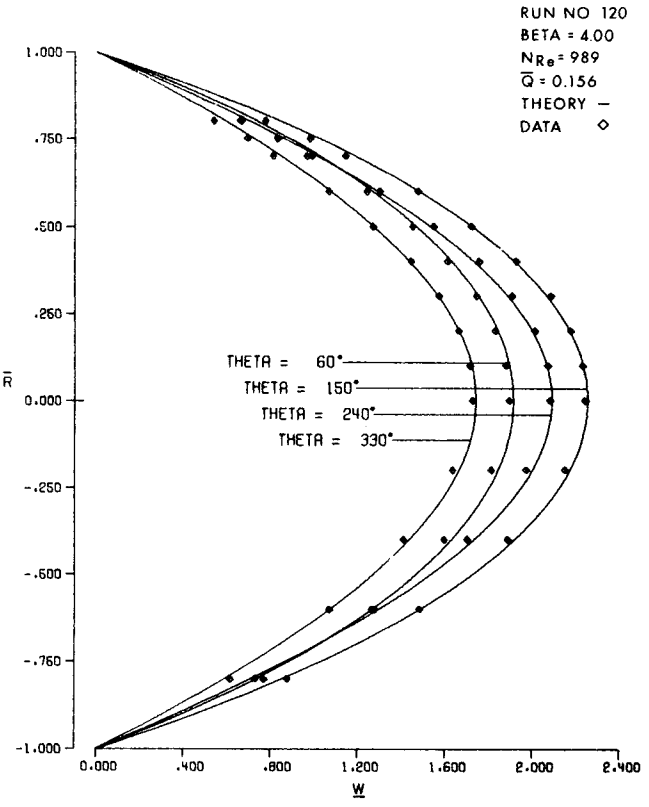

Fig. 9. Typical fully developed velocity profiles, pulsatile flow.

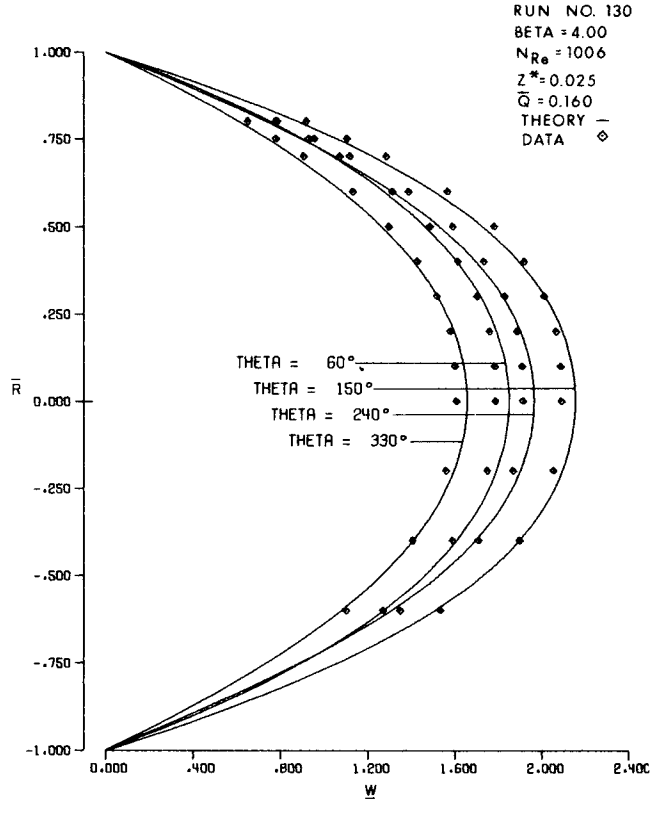

Fig. 11. Typical developing velocity profiles, pulsatile flow.

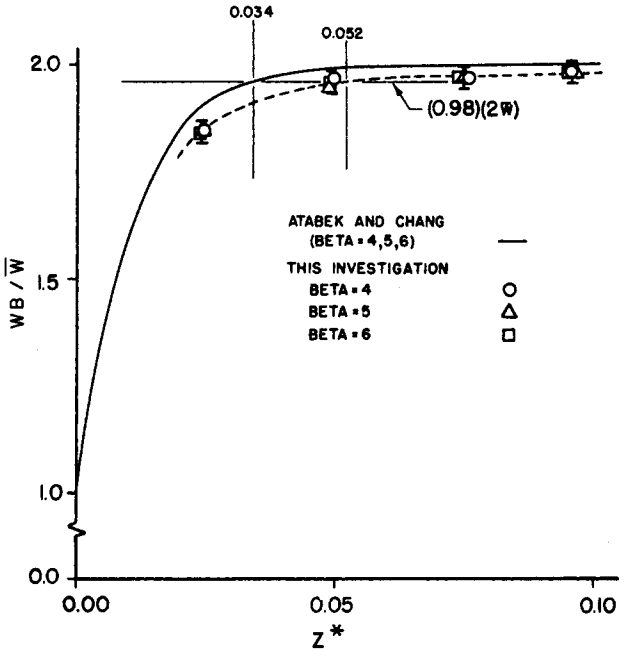

Fig. 12. Development length determination, pulsatile flow.

files in the fully developed region for pure oscillatory flow (zero mean velocity) at a rather high value of β. The normalization velocity in this case was chosen to be the center-line velocity at the time during the cycle when the maximum flow rate existed. Accuracy is quite good. The largest deviations occur near zero flow rate where acceleration is a maximum, and a small uncertainty in the sampling time leads to a large error in velocity. Further discussion of the oscillatory flow measurements has been presented elsewhere (*14*).

Figure 7 shows a typical pressure gradient for fully developed pulsatile flow. The digitized data trace is shown as is the result of the phase lag and amplitude correction. Figure 8 is a center-line velocity-time trace for the same run. Figure 9 presents the corresponding set of four velocity profiles across the tube with the normalization velocity being the mean velocity determined from the mass flow rate. The theory is that of Uchida (*20*). In Figure 10 the oscillatory component of the velocity is plotted for this run based on the same normalization velocity. Deviations from theory are accentuated due to the expanded scale.

A set of profiles for a run in the developing region is presented in Figure 11. It is obvious that the theory of Atabek and Chang (*3*) again predicts a more rapid development than was observed in this investigation.

The normalization velocity for all of the pulsatile flow runs (developing and fully developed) was between 1.0 and 1.2 ft./sec. while the maximum frequency of pulsation was near 0.4 Hz. A complete listing of the data is given elsewhere (*13*).

The entrance length for a steady pipe flow is normally defined as the point at which the center-line velocity reaches 99% of the fully developed value. The definition is more complicated for the case of a time-dependent flow. If an accurate determination is to be made on the basis of a 99% criterion, the velocity measurements must be accurate to a small fraction of a percent. Realizing the velocity measurement accuracy required to determine the entrance length as well as the complexity of defining the entrance length criterion for a time-dependent flow, the following simple definition will be employed based on average velocity in the tube and a 98% criterion:

$$\frac{\frac{1}{T}\int_0^T w(0,z,t)\,dt}{\frac{1}{T}\int_0^T w(0,\infty,t)\,dt} = \frac{\frac{1}{36}\sum_{m=1}^{36} w(0,z,m\Delta t)}{2\overline{w}} = \frac{WB}{2\overline{w}} = 0.98 \quad (2)$$

It can be shown (*13*) that the entrance length given by Atabek and Chang's solution using the above criterion is a function of both $\overline{Q}$ and β, but for the range of parameters covered in the present work it is virtually a constant. The prediction of Atabek and Chang and the results of the present investigation for developing pulsatile flow are shown in Figure 12. The experimental uncertainty of the data is shown on the curve (*13*). The theoretical prediction again yields a premature flow development.

ACKNOWLEDGMENT

The authors are grateful to Professor K. R. Purdy for his ingenious efforts during the design and construction of the flow system. This work was supported in part by the National Aeronautics and Space Administration.

NOTATION

β = $R(\omega/\nu)^{1/2}$
n = refractive index of the fluid
N_{Re} = $2R\overline{w}/\nu$
$\overline{Q}$ = ratio of the (maximum) unsteady flow rate to the mean flow rate
r = radial coordinate
R = tube radius
$\overline{R}$ = nondimensionalized (on radius) displacement from the tube center line in a horizontal plane
t = time
T = period of pulsation
$theta$ = time coordinate (one pulse cycle = 360°)
w = axial velocity
$\overline{w}$ = average (time average, mean) axial velocity
WB = $\frac{1}{36}\sum_{m=1}^{36} w(0,z,m\Delta t)$
W = $w/\overline{w}$
z = axial coordinate ($z = 0$ at entrance nozzle throat)
z^* = $\frac{z}{2R}\frac{1}{RE}$

Subscript

$\mathcal{L}$ = center line ($r = 0$)

Greek Letters

Δf_d = Doppler frequency shift
Δt = $T/36$
θ = angle between the reference beam and the scattering beam outside the tube (in air)
θ_f = angle between the reference beam and the scattering beam inside the tube (in the working fluid)
λ_o = radiation wavelength in a vacuum
ν = kinematic viscosity
ω = pulse frequency, radians/sec

LITERATURE CITED

1. Angus, J. C., D. L. Morrow, J. W. Dunning, Jr., and M. J. French, *Ind. Eng. Chem.*, **61**, 8 (1969).

2. "Fluid Meters—Their Theory and Application," 5th ed., p. 46, Am. Soc. Mech. Engrs., New York, N. Y. (1959).
3. Atabek, H. B., and C. C. Chang, *ZAMP*, **12**, 185 (1961).
4. Atabek, H. B., C. C. Chang, and L. M. Fingerson, *Phys. Med. Biol.*, **9**, 219 (1964).
5. Berman, N. S., and V. A. Santos, *AIChE J.*, **15**, 323 (1969).
6. Bettner, J. L., Ph.D. thesis, Purdue Univ., Lafayette, Ind. (1965).
7. Bond, R. L., Ph.D thesis, Univ. Arkansas, Fayetteville (1968).
8. Born, M., and E. Wolf, "Principles of Optics," pp. 652–656, Pergamon Press, Oxford (1965).
9. Christiansen, E. B., and H. E. Lemmon, *AIChE J.*, **11**, 995 (1965).
10. Combs, G. D., and D. A. Gilbrech, *Arkansas, Univ. (Fayetteville), Fluid Mech. Res. No. 1*, Prog. Rept. No. 2 (April, 1964).
11. Davis, D. T., *ISA Trans.*, **7**, 43 (1968).
12. Davis, W., Ph.D. thesis, Purdue Univ., Lafayette, Ind. (1966).
13 Denison, E B., Ph.D. thesis, Purdue Univ., Lafayette, Ind. (1970).
14. Denison, E. B., and W. H. Stevenson, *Rev. Sci. Instr.*, **41**, 1475 (1970).
15. Florio, P. J., Jr., and W. K. Mueller, *J. Basic Eng.*, **90**, 395 (1968).
16. Foreman, J. W., Jr., E. W. George, R. L. Jetton, R. D. Lewis, J. R. Thornton, and H. J. Watson, *IEEE (Inst. Elec. Electron. Eng.) J. Quantum Electron.*, **QE-2**, 260 (1966).
17. Goldstein, R. J., and W. F. Hagen, *Phys. Fluids*, **10**, 1349 (1967).
18. Goldstein, R. J., and D. K. Kreid, *J. Appl. Mech.*, **34**, 813 (1967).
19. M. J. Rudd, *J. Sci. Instr. (J. Phys. E)*, **2**, 55 (1969).
20. Uchida, S., *ZAMP*, **7**, 403 (1956).
21. Yeh, Y., and H. Z. Cummins, *Appl. Phys. Letters*, **4**, 176 (1964).

Optimal Operation of Regeneratively Cooled Fixed Bed Reactors

GEORGE R. GAVALAS

Chemical Engineering Laboratory
California Institute of Technology, Pasadena, California 91109

SCOPE

Exothermic catalytic processes including hydrocarbon oxidations consist of multiple reactions such as

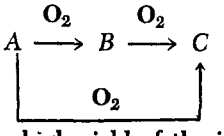

The production of a high yield of the intermediate B and the prevention of catalyst damage set an upper limit on the allowable temperature. Because relatively high temperatures are needed to obtain reasonable conversions, the two opposing requirements suggest the existence of an optimum temperature profile along the reactor. Such optimum temperature profiles have been derived theoretically, and reference (*1*) gives the most recent results and summarizes the previous work.

The practical implementation of these profiles, however, would require rather elaborate heat transfer arrangements. Thus, the heat transfer methods used in industrial reactors maintain the temperature within allowable limits but do not attempt to impose any detailed temperature profile. Such arrangements include the tube- and shell-reactor heat exchanger, the dilution of the feed with an inert serving as a heat sink, the multistage reactor with intermediate cooling, and the fluidized bed reactor.

In a previous paper (*2*) we proposed regenerative cooling as another method for temperature control in exothermic catalytic reactions. Essentially, the heat of reaction is absorbed by the solid catalyst during one half of the cycle. During the other half, the catalyst is cooled by internal circulation of a gas that can be one of the reactants. This type of regenerative operation is distinct from the regeneration of a catalyst that has been deactivated by coking or a feed poison. Regenerative operation relative to heat transfer has so far been applied only to such endothermic processes as the production of ethylene and acetylene (*3*), and butene (*4*). As already mentioned, at steady state it is difficult to achieve the optimum yields because of difficulties in implementing the optimum temperature profiles. The present paper investigates the possibility of achieving yields close to the optimum steady state by optimizing the regenerative mode of operation. The implementation of the optimal policies by practical means is given special attention.

SUMMARY

A regeneratively cooled fixed bed reactor, shown in Figure 1, consists of two sections alternating roles as reactor and heat regenerator by periodic flow reversals. The reactor can have any desired diameter because the cooling occurs strictly by regeneration. The system possesses four control variables that can be adjusted for optimal operation. The first is the temperature profile in the reacting section at the beginning of each cycle and is implemented during regeneration. The second is the temperature of the feed to the reacting section as a function of time. The third is the catalyst activity profile and can be implemented by mixing the catalyst with an inert solid. The last is the period of cycling, that is, the time interval between flow reversals. These four variables are not available in steady state designs.

Correspondence concerning this article should be addressed to Prof. George R. Gavalas.